Supporting Information

Cooperative phenomenon of vapochromism and proton conduction of luminescent Pt(II) complexes for the visualisation of proton conductivity

Atsushi Kobayashi,[a]* *Shin-ichiro Imada,*[a] *Dongjin Wang,*[b] *Yuki Nagao,*[b] *Masaki Yoshida,*[a] *and Masako Kato*[a]*

[a] *Department of Chemistry, Faculty of Science, Hokkaido University, North-10 West-8, Kita-ku, Sapporo, Hokkaido 060-0810, Japan*

[b] *School of Materials Science, Japan Advanced Institute of Science and Technology, 1–1 Asahidai, Nomi, Ishikawa 923-1292, Japan*

Contents

Table S1. Crystal parameters and refinement data.

Complex	***o*-Pt**	***o*-Pt·HCl**	***o*-Pt·MeOH**
CCDC No.	1975537	1975539	1975538
T / K	150(2)	150(2)	150(2)
Formula	$C_{20}H_{14}Cl_2N_4Pt \cdot H_2O$	$C_{20}H_{14}Cl_2N_4Pt \cdot 1.25HCl \cdot 3H_2O$	$C_{20}H_{14}Cl_2N_4Pt \cdot CH_3OH$
Formula weight	595.36	675.97	615.40
Crystal system	*monoclinic*	*triclinic*	*triclinic*
Space group	$P2_1/c$	P-1	P-1
a / Å	5.3046(1)	13.5911(4)	8.0185(1)
b / Å	21.6781(3)	14.4864(5)	10.5928(2)
c / Å	15.9776(2)	14.6981(4)	13.0124(3)
α / °	90	99.605(2)	69.402(2)
β / °	94.542(1)	101.408(2)	86.254(2)
γ / °	90	117.546(3)	72.413(2)
V / Å ^{3}	1831.55(5)	2401.44(14)	985.20(4)
Z	4	2	2
D_{cal} / g cm^{-3}	2.155	1.858	2.051
Reflections collected	9949	27916	10329
Unique reflections	3262	8585	3525
R_{int}	0.0449	0.0509	0.0311
GOF	1.035	1.044	0.740
R_1 ($I > 2\sigma$ (I)) [a]	0.0432	0.0467	0.0261
wR_2 [b]	0.1223	0.1302	0.0801

[a] $R_1 = \Sigma||F_o| - |F_c||/\Sigma|F_o|$. [b] $wR_2 = [\Sigma w(F_o^2 - F_c^2)/ \Sigma w(F_o)^2]^{1/2}$, $w = [\sigma_c^2(F_o^2) + (xP)^2 + yP]^{-1}$, $P = (F_o^2 - 2F_c^2)/3$.

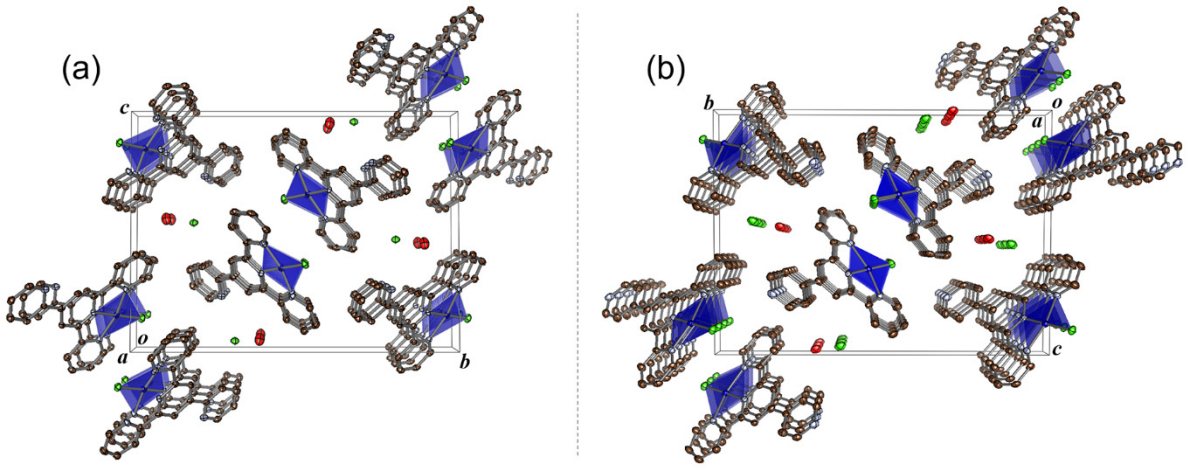

Figure S1. Packing diagrams of (a) ***o*-Pt** and (b) ***p*-Pt** viewed along the *a* axis.

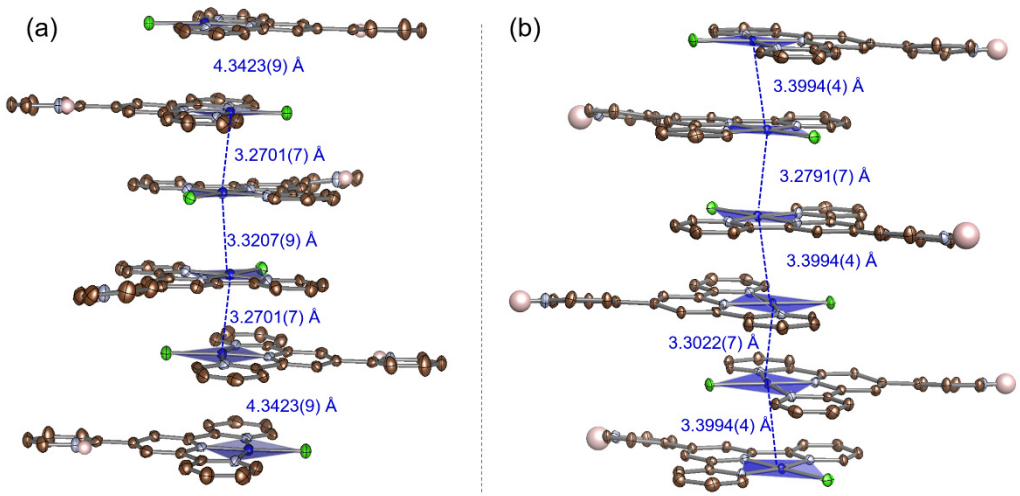

Figure S2. Stacking structures of (a) ***o*-Pt·HCl** and (b) ***p*-Pt·HCl**. Values shown in blue are the intermolecular Pt···Pt stacking distance between the adjacent molecules. The values are the intermolecular Pt···Pt distances.

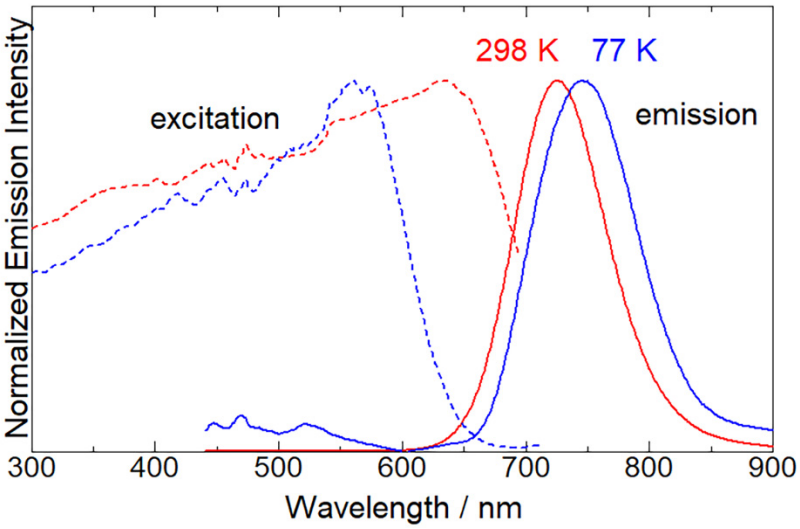

Figure S3. Excitation (dotted lines) and emission (solid lines, λ_{ex} = 400 nm) spectra of **o-Pt·HCl** at 298 (red) and 77 K (blue) in the solid state.

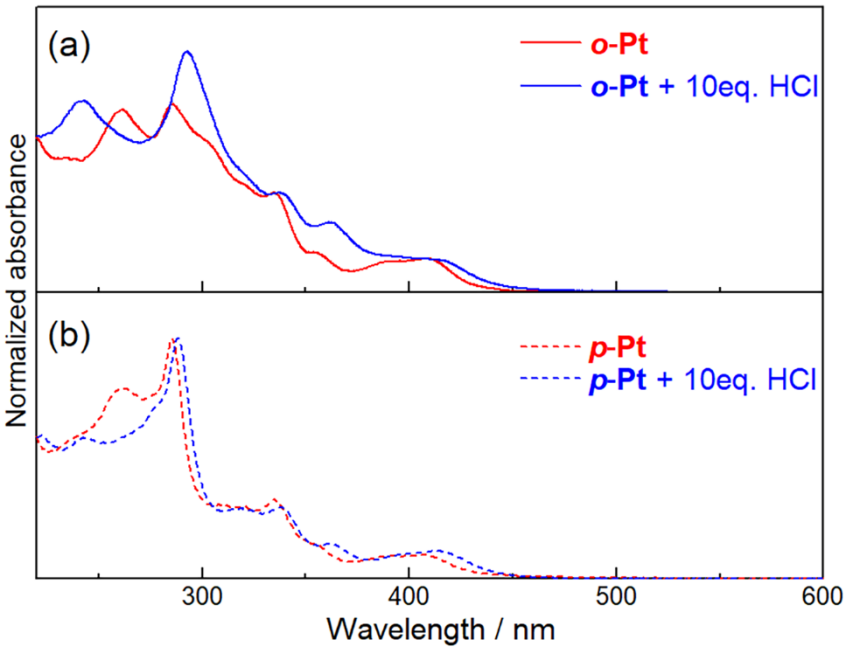

Figure S4. UV-Vis absorption spectra of (a) ***o*-Pt** and (b) ***p*-Pt** in MeOH solution in the absence (red lines) and presence of 10 eq. HCl (blue lines) at 293 K.

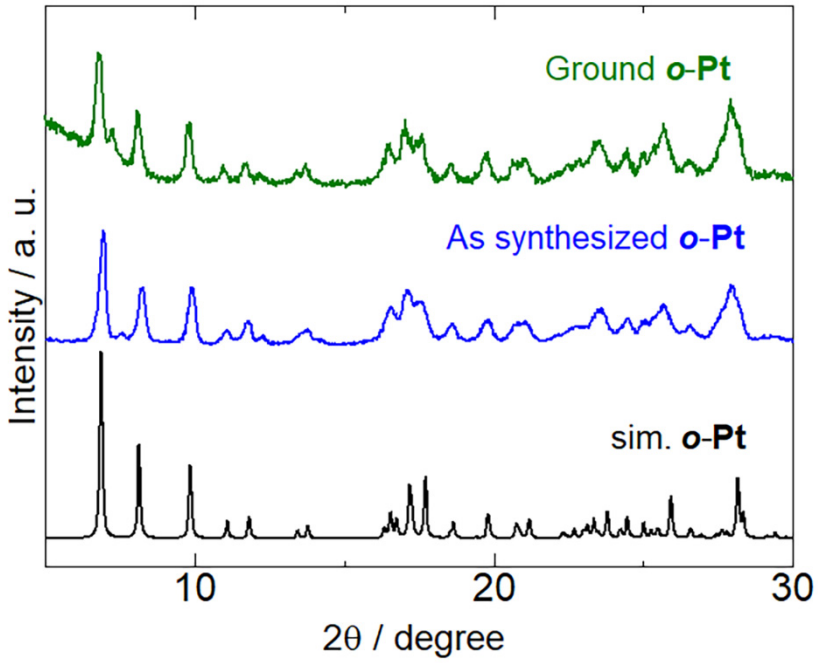

Figure S5. Change of the PXRD pattern of ***o*-Pt** by manual grinding. The bottom line shows the simulation pattern calculated from the crystal structure of ***o*-Pt**.

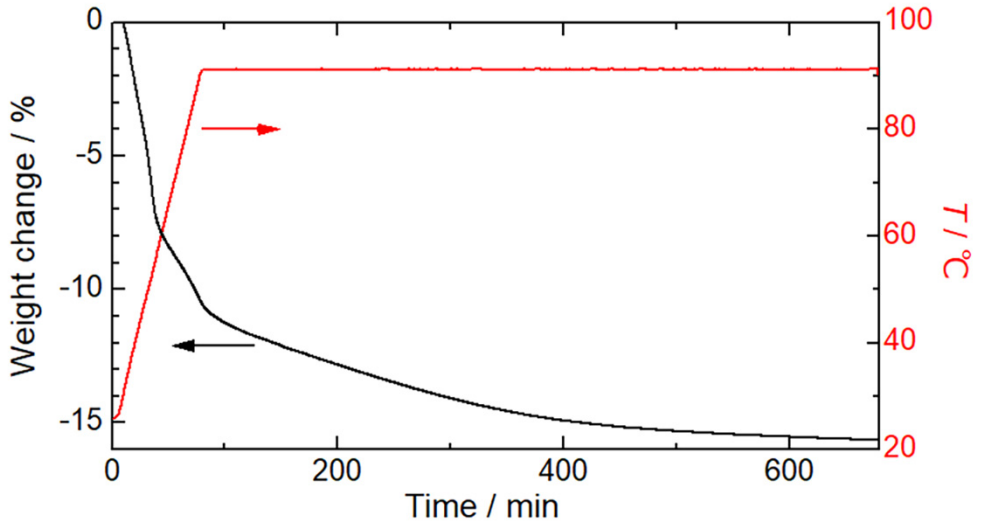

Figure S6. TGA curve of HCl-vapour-exposed ***o*-Pt** by heating at 90 °C in Ar flow (0.3 L/min). Observed weight loss after heating at 90 °C for 8 h (-15.63%) was almost agreed to the mass percent of HCl and hydrated water molecules of ***o*-Pt·HCl** (1.25 HCl and $3H_2O$ per one Pt(II) cation, 14.7%).

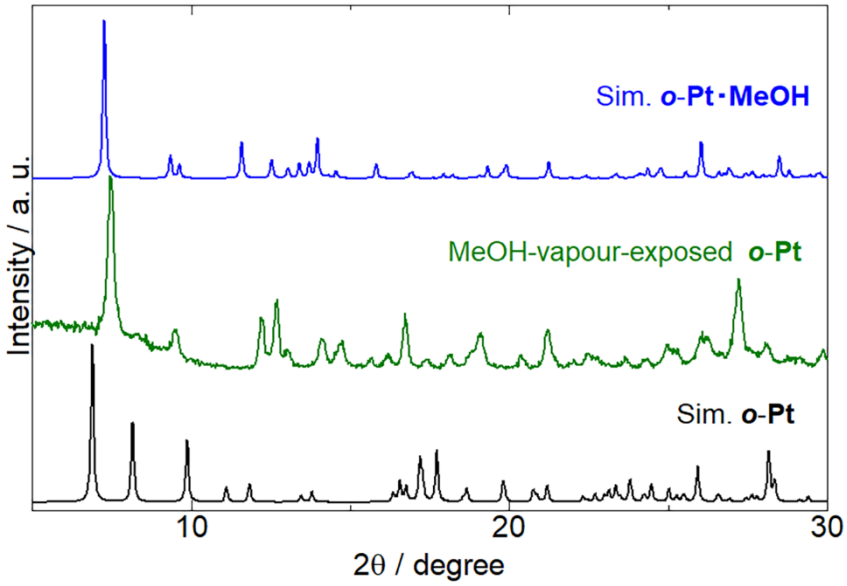

Figure S7. Change of the PXRD pattern of ***o*-Pt** under MeOH vapor. Bottom and top lines show the simulation patterns calculated from the crystal structures of ***o*-Pt** and ***o*-Pt·MeOH**.

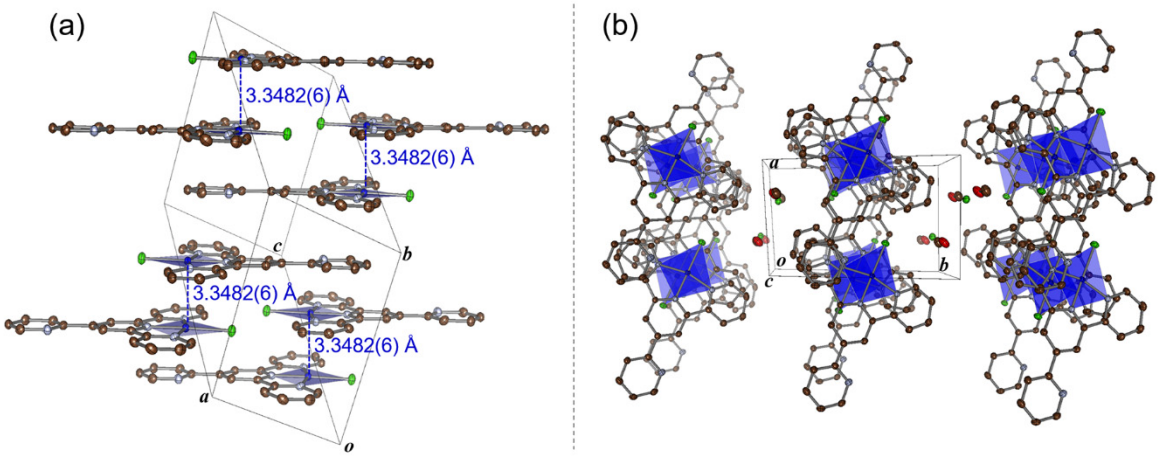

Figure S8. Crystal structure of MeOH-solvated crystal ***o*-Pt·MeOH**. (a) Stacking structure and (b) Packing diagram viewed along the *c* axis. The values in panel (a) are the intermolecular Pt···Pt distances.

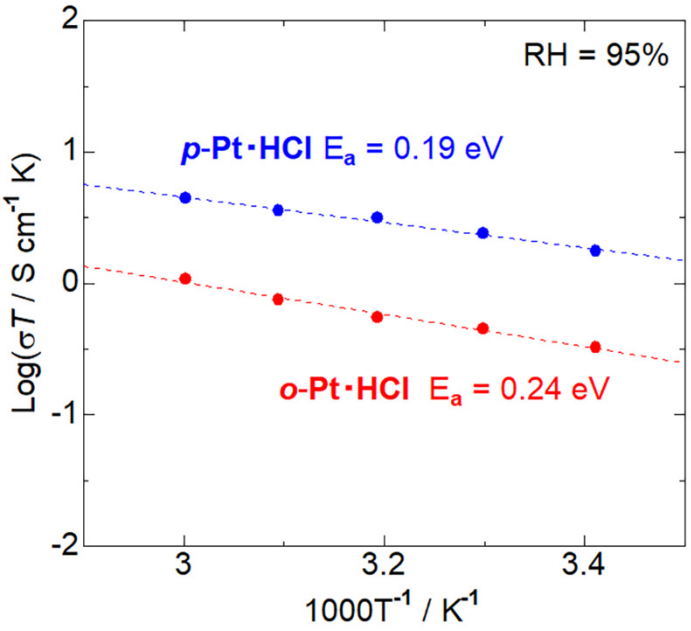

Figure S9. Arrhenius plots of proton conductivities of ***o*-Pt·HCl** (red) and ***p*-Pt·HCl** (blue) in the range of 293–333 K at 95% RH.

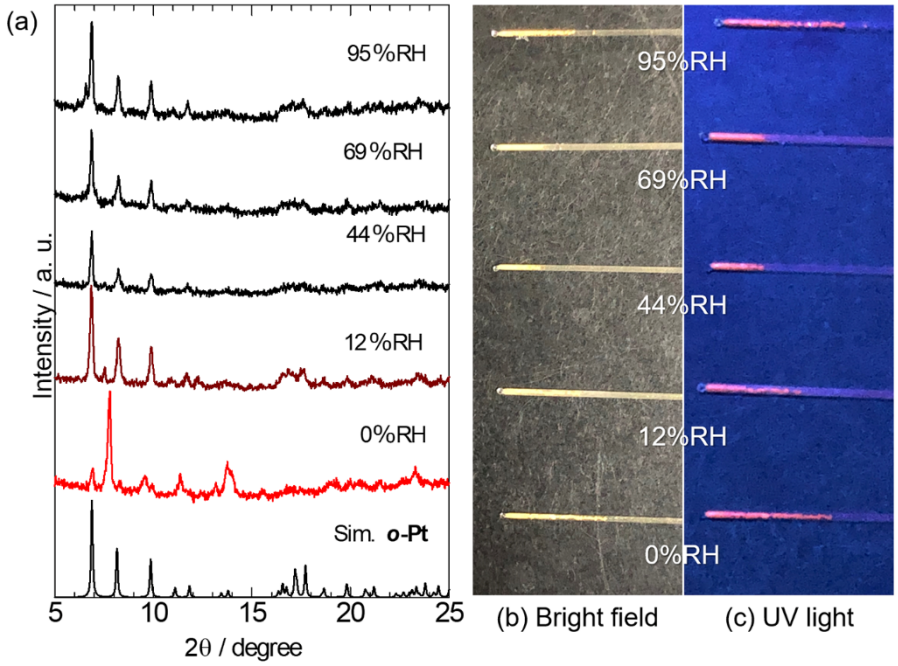

Figure S10. (a) RH-dependence of the PXRD pattern of ***o*-Pt** and photographs under (b) bright field and (c) UV light.